SUPPLEMENTARY FIGURE LEGENDS

Supplementary Figure S1. Phenotypic characterization panel of the PDX model. Hematoxylin and eosin staining of patients´ tumors and PDX tumor mice at passage 0 (p0), passage 1 (p2) and passage 2 (p2), (magnification ×200).

Supplementary Figure S2. Study flow diagram. Abbreviations: NSCLC, non–small cell lung carcinoma; PDX, patient-derived xenograft.

Supplementary Figure S3. Effect of different treatments on tumor size and on tumor necrosis in patient-derived xenograft PDX6 mice. (**A**) Tumor growth curves are expressed as a percentage of the change of initial tumor volume, which was considered as 100%. Each point represents a measurement day given as the mean ± SEM of the tumor volume of the mice of each group. (**B**) Mice were sacrificed after six weeks and the tumor volume was measured. Results are shown as mean ± SEM of the tumor volume of the mice of each group. Statistical significance is indicated ($p \leq 0.05$) and was analyzed by the Kruskal-Wallis non-parametric test. Post hoc between-group comparisons were made with the Mann-Whitney test. (**C**) The necrosis index is expressed as a percentage of necrotic areas. Values represent the percentage (mean ± SEM). Statistical significance is indicated ($p \leq 0.05$) and was analyzed by the Kruskal-Wallis non-parametric test. Post hoc between-group post hoc comparisons were made with the Mann-Whitney test.

Supplementary Figure S4. Tumor PDX4 histologies and inflammatory response associated with tumor regression in response to anti-PD-1 treatments in PDX4 and PDX6. (**A**) Selection of representative histological hematoxylin and eosin-stained images (×1) of each PDX4 treatments group, showing evident necrotic areas. (**B**) Representative hematoxylin and eosin-stained image of a tumor from a PDX4 mouse treated with anti-PD-1 → cisplatin (sequential). Necrotic areas showing polymorphonuclear cells, macrophages and dead epithelial cells, ×1. (**C**) Zoomed image of the necrotic zone marked with a square in panel B, where polymorphonuclear cells are observed, ×100. (**D**) Representative hematoxylin and eosin-stained image of a tumor from a PDX6 mouse treated with anti-PD-1. Necrotic areas not showing polymorphonuclear cell infiltration, only remnants of dead epithelial cells, ×1. (**E**) Zoomed image of the necrotic zone marked with a square in panel D, ×100.

Supplementary Figure S5. Human cells in xenografts. (**A**) Flow cytometry analysis of the immune component in blood and in tumor homogenates. Representative dot plot showing human CD45 (hCD45) *versus* murine CD45 (mCD45.1) staining of peripheral blood of a PDX4 mouse. (**B**) Representative flow cytometry analysis of homogenized tumors, using hCD45. Cells were stained with antibodies against human, hCD45 (red) and murine, mCD45 (purple) leukocytes. (**C**) Representative flow cytometry analysis of the inflammatory component from fluid collected from a PDX4 tumor treated with anti-PD-1, as in B. (**D**) *In situ* hybridization of Alu-sequences, revealing the presence of human cells (stained dark brown) throughout the tumor tissue, with the exception of the

matrix and the endothelium, which is murine-derived (not-stained, light blue) in PDX4 tumor, ×20; (**E**) PDX4 tumor, ×50. (**F**) Negative immunohistochemistry for surface markers on lymphocytes in a PDX tumor, **1**) human CD45 (hCD45), **2**) hCD3, **3**) hCD4, **4**) hCD20; ×20.

Supplementary Figure S6. Neutrophil morphology. (**A**) Schematic representation of the typical morphology of murine hypersegmented neutrophils (modified from Pillay, J., Tak, T., Kamp, V.M., Koenderman, L. Immune suppression by neutrophils and granulocytic myeloid-derived suppressor cells: similarities and differences. *Cell Mol Life Sci* **70**, 3813–3827, doi:10.1007/s00018-013-1286-4 (2013). (**B**) Liquid cytology (*ThinPrep,* Cytyc Corporation; Boxborough, MA, USA) of the exudate from a tumor treated with anti-PD-1 in our study, showing neutrophils with multilobed and hypersegmented nuclei (magnification ×100), with one of them shown in more detail in (**C**) (magnification ×150). (**D**) Isolated peripheral neutrophil incubated in vitro with anti-PD-1 (50 μg/ml), whose nuclear morphology without staining is shown in an immunofluorescence detection image. (**E**) The multilobed, hypersegmented nucleus of the neutrophil previously shown in (**D**) is displayed here with a negative photo filter.

Supplementary Figure S7. Detection of neutrophils and nitrotyrosine in PDX tumors that received anti-PD-1 treatment and detection of anti-PD-1 in the original patient tumor tissue. (**A**) Representative images of the expression and localization of myeloperoxidase (red) and nitrotyrosine (green) by confocal microscopy in PDX4 tumors treated with anti-PD-1 monotherapy. Nuclei were stained with TO-PRO-3 (blue). Merged image corresponding to the necrotic areas reveals co-localization (yellow) of myeloperoxidase and nitrotyrosine, marked by white arrows. Scale bars, 30 μm. (**B**) Double immunofluorescence staining of myeloperoxidase and nitrotyrosine in PDX tumors. Representative merged images of the expression and localization of myeloperoxidase (red) and nitrotyrosine (green) by confocal microscopy in PDX tumors from control group, cisplatin-treated and anti-PD-1 and cisplatin (sequential) treated group. Nuclei were stained with TO-PRO-3 (blue). Co-localization (yellow) of myeloperoxidase and nitrotyrosine is marked by white arrows. Scale bars, 30 μm. (**C**) Detection of anti-PD-1 treatment antibody binding to infiltrated cells and necrotic areas of the original patient tumor tissue. Representative images of the location of anti-PD-1 bound (red) using confocal microscopy. Nuclei were stained with TO-PRO-3 (blue) and the images were merged. Scale bars, 100 μm.

Supplementary Figure S8. Anti-PD-1 antibody binding sites on neutrophil cell membrane surface. Representative confocal microscopy images of anti-PD-1 bound to PD-1 receptor (green color) on isolated murine neutrophils. The PD-1 active protein (in red) is bound to anti-PD-1 which is in turn is attached to the neutrophil through fragment crystallizable (Fc)-gamma receptors (FcγRs). Right panel shows merged images of co-localization (yellow color) of both receptors in the neutrophil. (**A**) Scale bars, 10 μm; (**B**) Scale bars, 20 μm; (**C**) Scale bars, 20 μm.

SUPPLEMENTARY MATERIAL

Research Article

TITLE

Effects of anti-PD-1 immunotherapy on tumor regression: insights from a patient-derived xenograft model.

AUTHORS

Asunción Martín-Ruiz[1,2], Carmen Fiuza-Luces[3], Esther Martínez-Martínez[1,4], Clemente F. Arias[5], Lourdes Gutiérrez[1], Manuel Ramírez[6], Paloma Martín-Acosta[7], Maria José Coronado[8], Alejandro Lucia[2,3] and Mariano Provencio[1*].

***Correspondence:** Dr. Mariano Provencio, mprovenciop@gmail.com

SUPPLEMENTARY MATERIAL

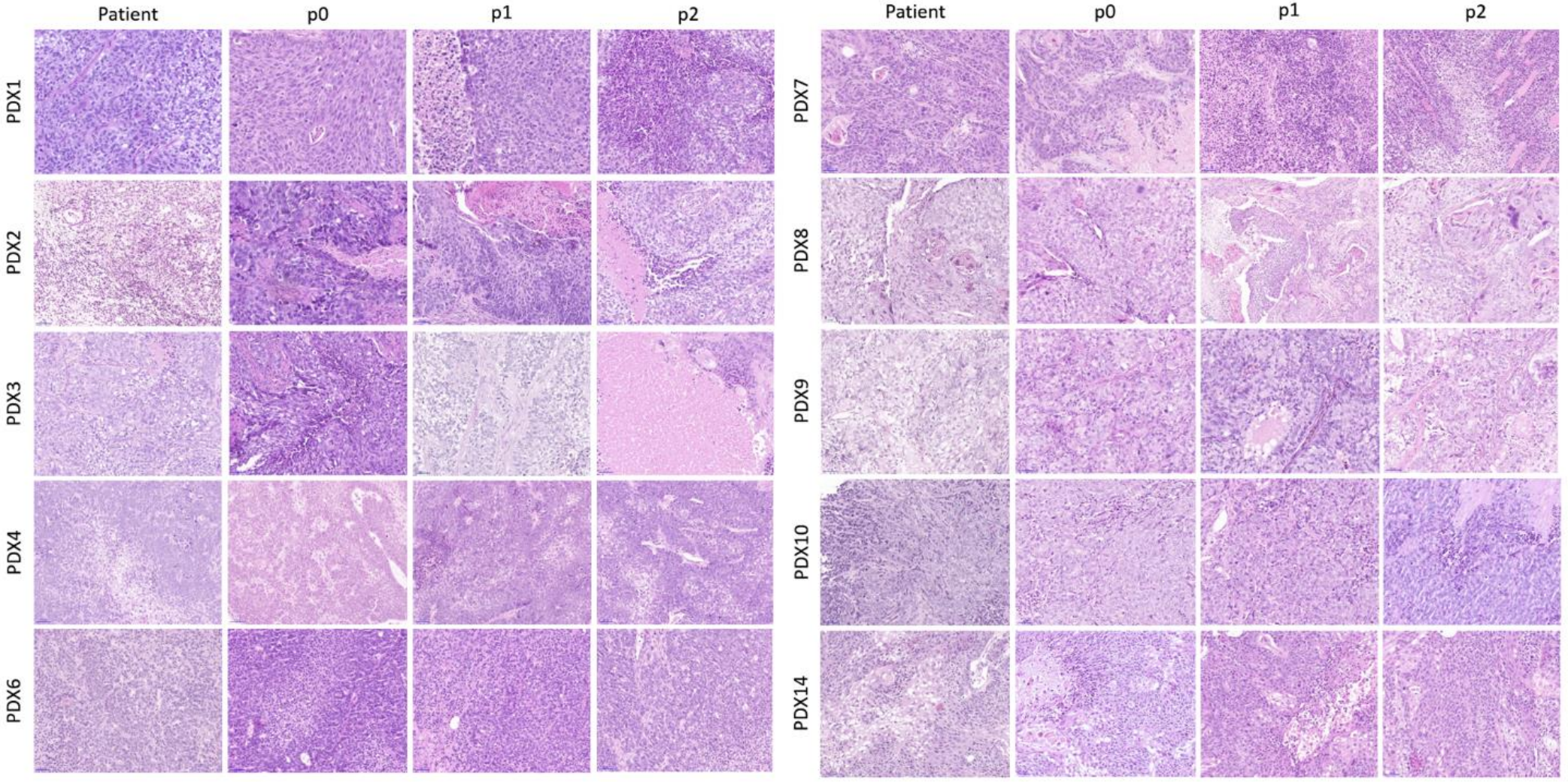
Patient
p0
p1
p2
PDX1
PDX2
PDX3
PDX4
PDX6
Patient
p0
p1
p2
PDX7
PDX8
PDX9
PDX10
PDX14

Figure S1

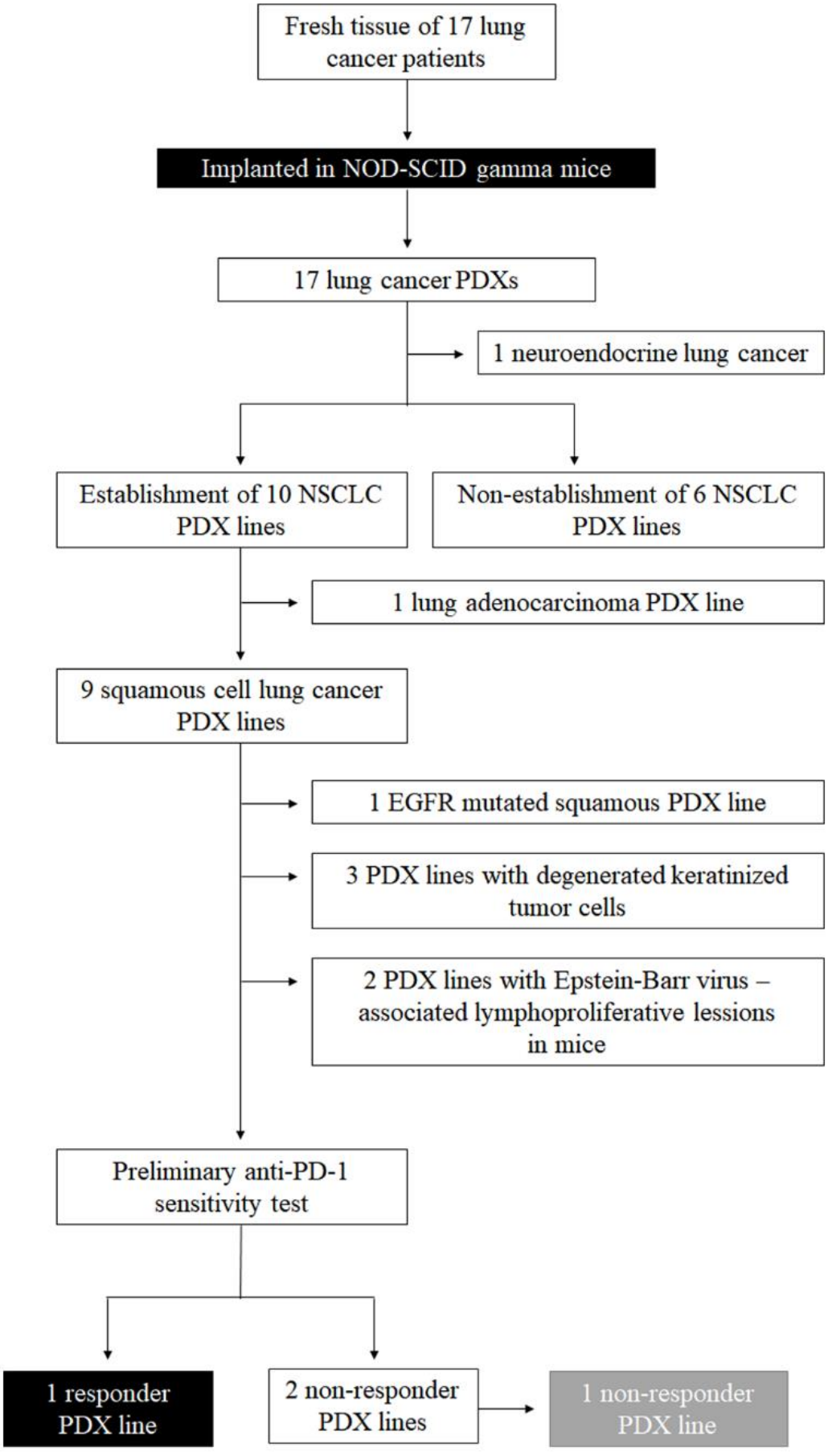
Fresh tissue of 17 lung cancer patients
Implanted in NOD-SCID gamma mice
17 lung cancer PDXs
1 neuroendocrine lung cancer
Establishment of 10 NSCLC PDX lines
Non-establishment of 6 NSCLC PDX lines
1 lung adenocarcinoma PDX line
9 squamous cell lung cancer PDX lines
1 EGFR mutated squamous PDX line
3 PDX lines with degenerated keratinized tumor cells
2 PDX lines with Epstein-Barr virus – associated lymphoproliferative lessions in mice
Preliminary anti-PD-1 sensitivity test
1 responder PDX line
2 non-responder PDX lines
1 non-responder PDX line

Figure S2

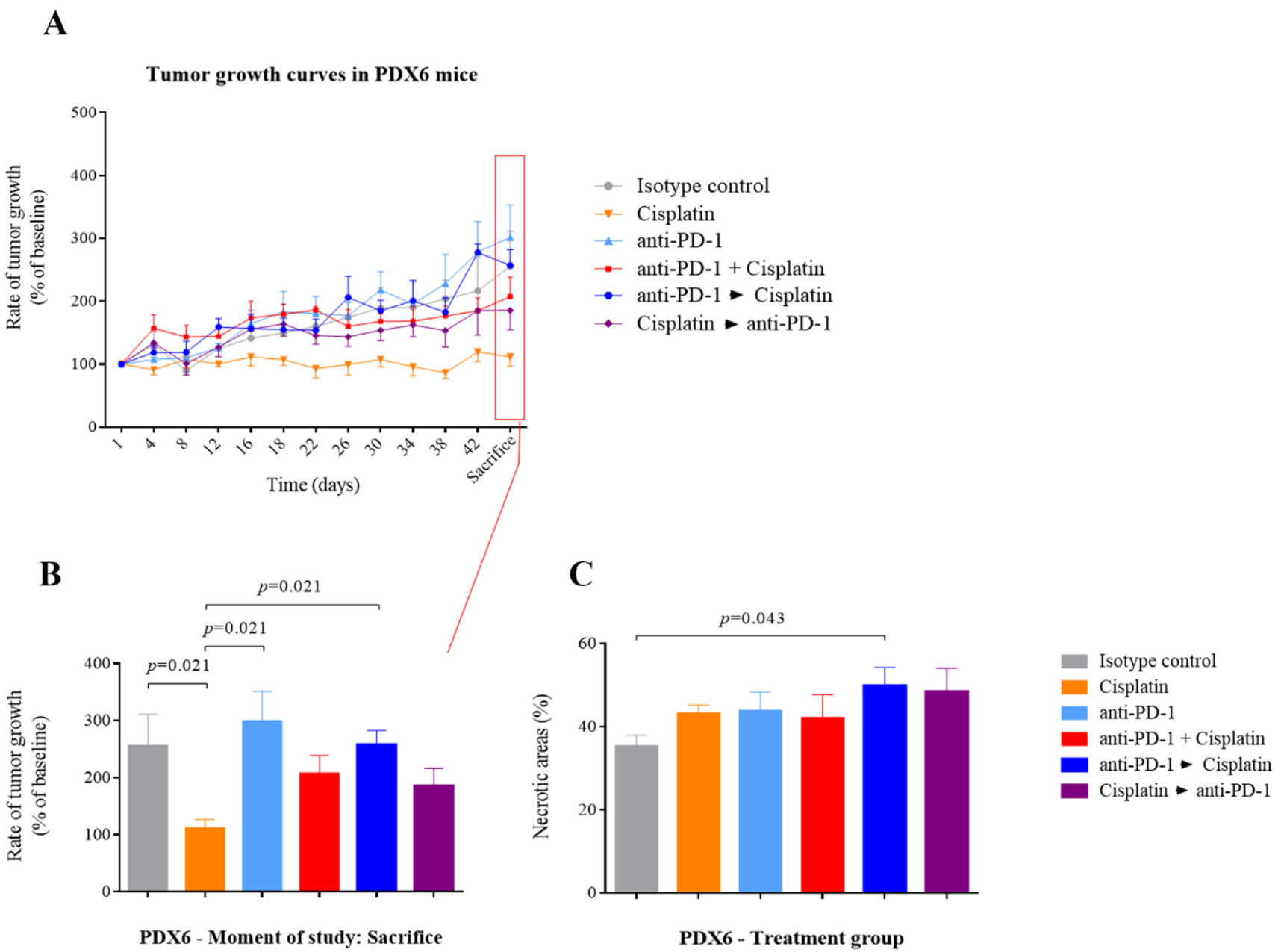
A
Tumor growth curves in PDX6 mice
Rate of tumor growth (% of baseline)
Time (days)
Sacrifice
Isotype control
Cisplatin
anti-PD-1
anti-PD-1 + Cisplatin
anti-PD-1 ► Cisplatin
Cisplatin ► anti-PD-1
B
p=0.021
p=0.021
p=0.021
Rate of tumor growth (% of baseline)
PDX6 - Moment of study: Sacrifice
C
p=0.043
Necrotic areas (%)
PDX6 - Treatment group

Figure S3

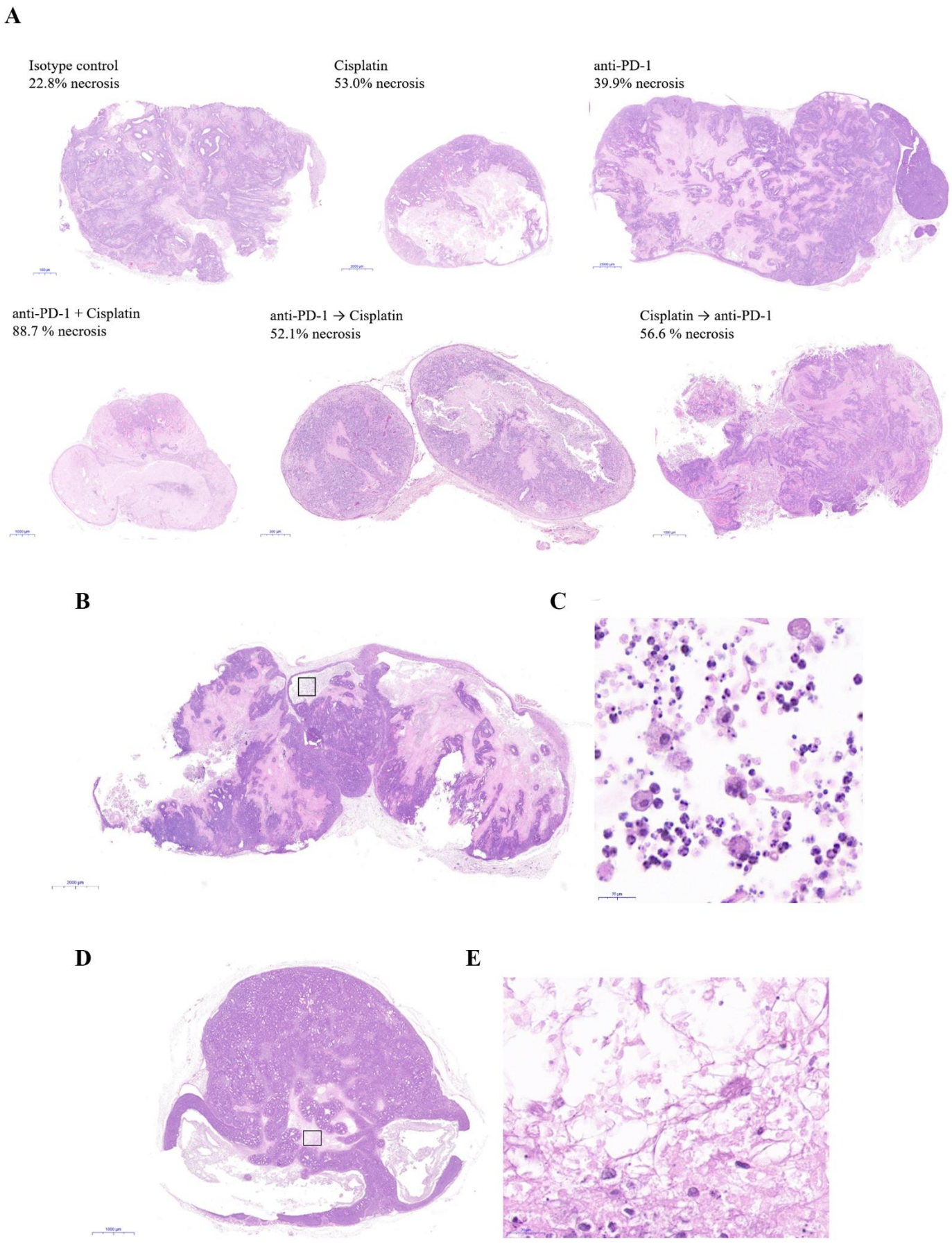
A
Isotype control
22.8% necrosis
Cisplatin
53.0% necrosis
anti-PD-1
39.9% necrosis
anti-PD-1 + Cisplatin
88.7 % necrosis
anti-PD-1 → Cisplatin
52.1% necrosis
Cisplatin → anti-PD-1
56.6 % necrosis
B
C
D
E

Figure S4

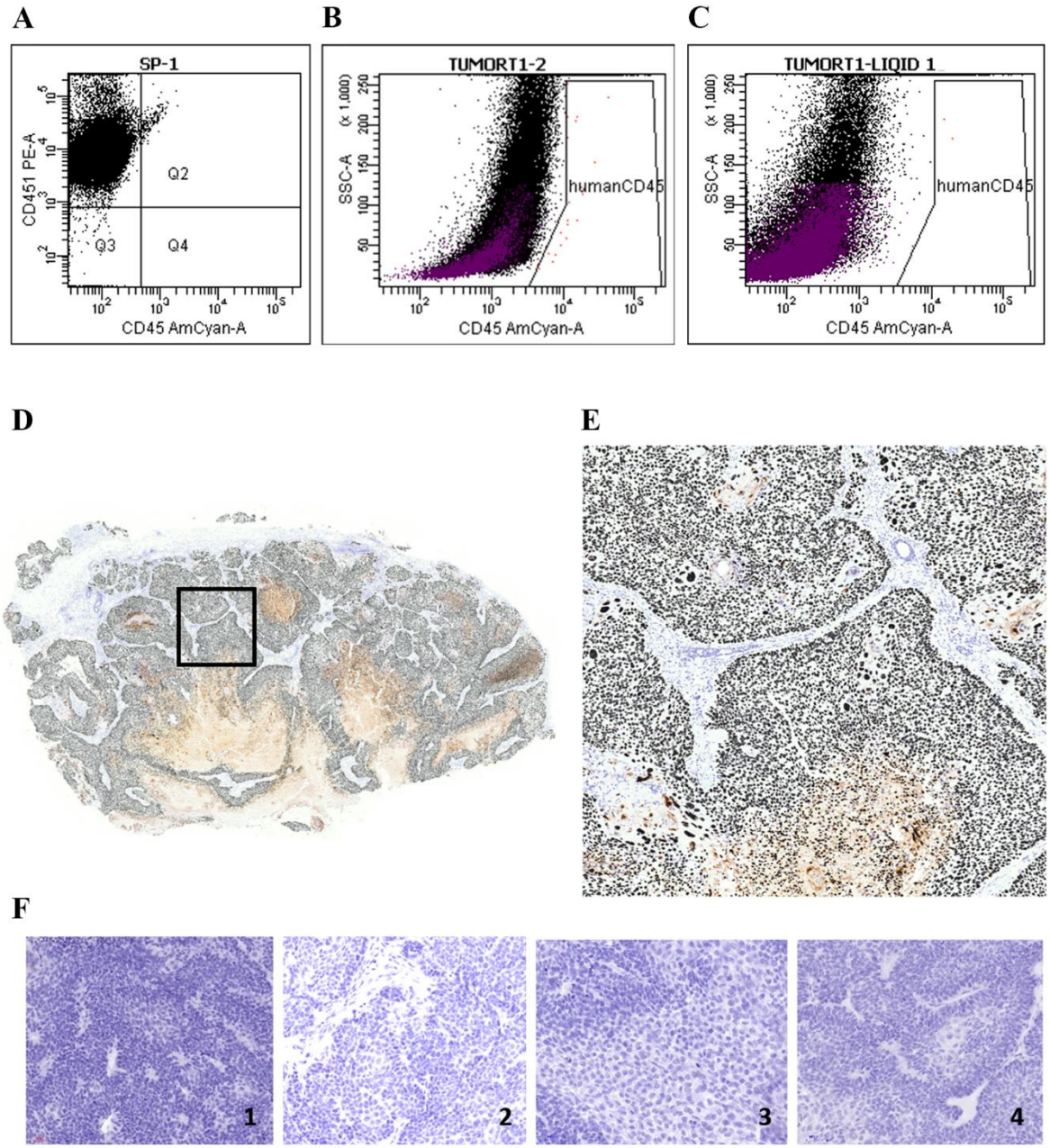
A
SP-1
CD451 PE-A
Q2
Q3
Q4
CD45 AmCyan-A
B
TUMORT1-2
SSC-A
humanCD45
CD45 AmCyan-A
C
TUMORT1-LIQID 1
SSC-A
humanCD45
CD45 AmCyan-A
D
E
F
1
2
3
4

Figure S5

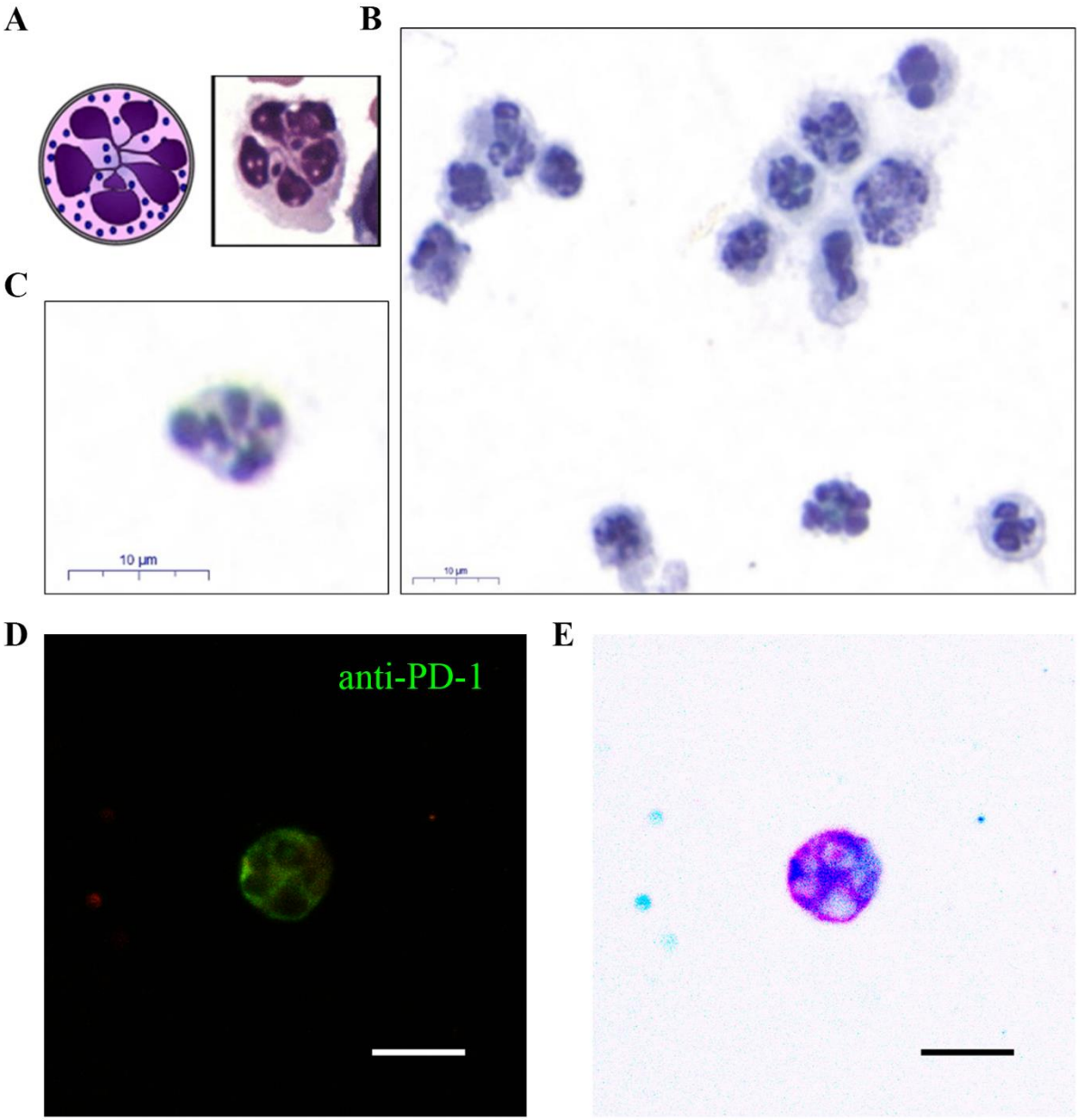

Figure S6

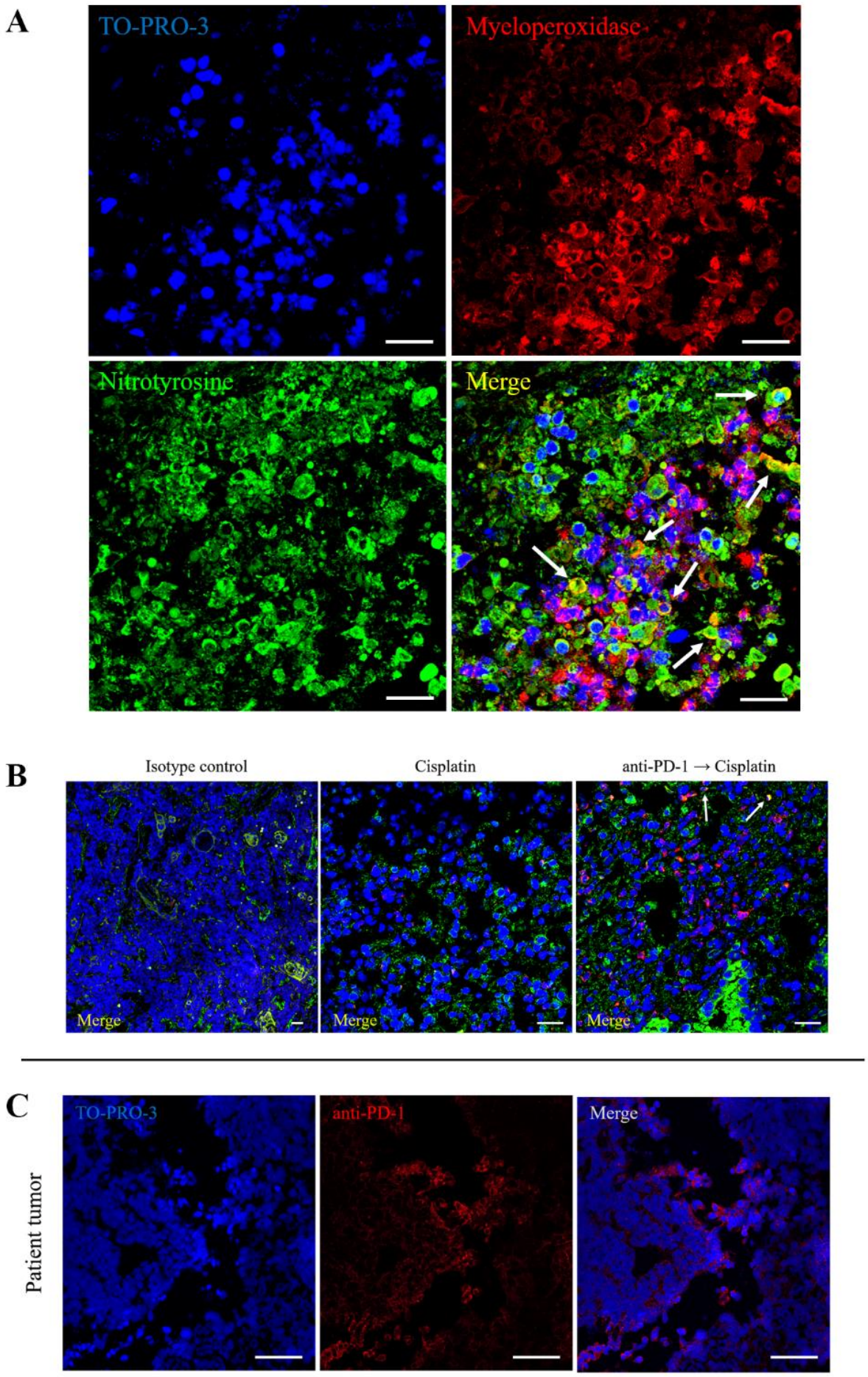
A
TO-PRO-3
Myeloperoxidase
Nitrotyrosine
Merge
B
Isotype control
Cisplatin
anti-PD-1 → Cisplatin
Merge
Merge
Merge
C
Patient tumor
TO-PRO-3
anti-PD-1
Merge

Figure S7

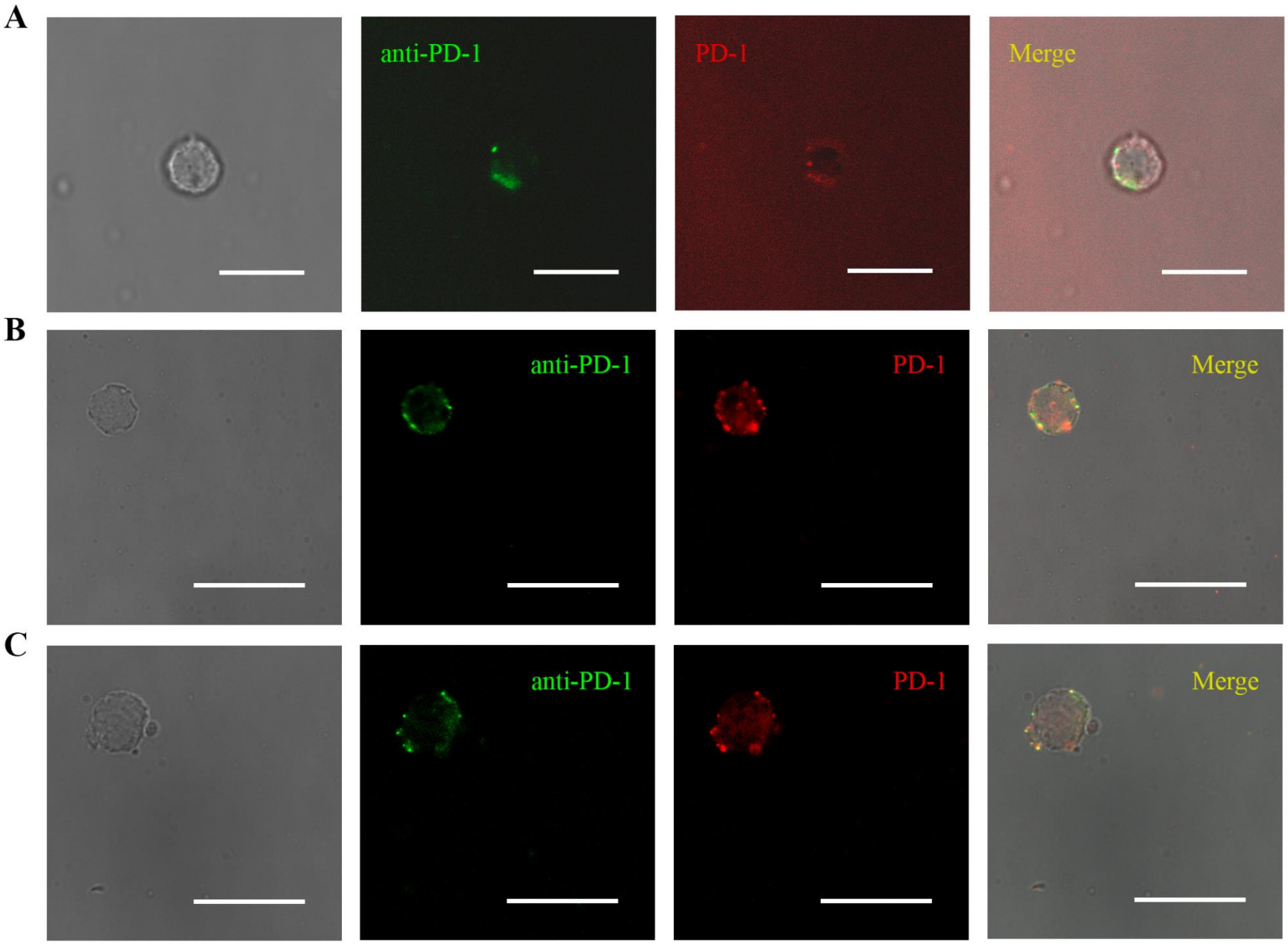

Figure S8

Supplementary text file S1

Establishment of a human squamous NSCLC PDX model

Female 8-week-old NOD-SCID gamma (NOD.Cg-*Prkdc*^{scid} *Il2rg*^{tm1Wjl}/SzJ) mice were purchased from Charles River Laboratories (Chatillon-sur-Chalaronne, France). Mice were transplanted with a direct surgically obtained tumor sample from patients with NSCLC using the following protocol. The specimen was sliced into fragments (~3 mm × 2 mm) and two pieces were implanted subcutaneously into the flanks (bilateral grafts) of each host mouse (passage 0 or p0) under inhalation anesthesia (sevoflurane in oxygen, Sevorane). After transplant, tumor growth was monitored and, whenever palpable, the volume was measured with a caliper (AA846R, Aesculap AG, Tuttlingen, Germany) twice weekly using the following formula: $(4\pi/3) \times (w/2)^2 \times (l/2)$, where w = width and l = length. When the tumor volume reached ~1 cm^3, the mice were sacrificed by CO_2 inhalation. A portion of the harvested tumor was used for phenotype and molecular analyses to verify that the xenograft model was histopathologically stable, and another portion was harvested and serially re-engrafted to maintain the *in vivo* PDX line during subsequent passages (termed p1, p2, etc.). Several NSCLC PDX lines were established, and those lines fulfilling the following criteria were selected: squamous histology, not having driver mutations, and maintenance of the original tumor characteristics throughout the passages.

Preliminary test of response to anti-PD-1 therapy

To evaluate the response of the PDX model to immunotherapy, a preliminary test was performed based on changes to tumor volume, which would allow for the detection of responders *versus* non-responders. Groups of three mice (p1) were administered with anti-PD-1 therapy (nivolumab [Opdivo®, Bristol-Myers Squibb, Princeton, NJ, USA is a fully human immunoglobulin G4 (hIgG4, Crown Bioscience, Inc. [Santa Clara, CA, USA]) PD-1 immune checkpoint inhibitor antibody that disrupts the interaction of PD-1 with its ligands PD-L1 and PD-L2, blocking the immune response], 150 μg) or an equivalent dose of an irrelevant hIgG4 by intra-peritoneal (i.p.) injection twice weekly for 3 consecutive weeks. Responder mice were selected and maintained through consecutive passages.

Supplementary Table S1. Primary antibodies used for different immunodetection techniques

Antibody	Supplier	Clone	Type	Species	Uses	System	Dilution
TTF-1	Dako	8G7G3/1	mAb, mouse	Human	IHC	Omnis Dako	1:200
CD56	Dako	123C3	mAb, mouse	Human	IHC	Omnis Dako	1:50
Synaptophysin	Dako	DAK-SYNAP	mAb, mouse	Human	IHC	Omnis Dako	*Ready-to-use*
Napsin-A	Novocastra	IP64	mAb, mouse	Human	IHC	Leica	1:500
p40	Dako	BC28	mAb, mouse	Human	IHC	Ventana (Roche)	1:500
p63	Dako	DAK-p63	mAb, mouse	Human	IHC	Omnis Dako	*Ready-to-use*
CK-5/6	Dako	D5/16 B4	mAb, mouse	Human	IHC	Omnis Dako	*Ready-to-use*
CD45	Dako	2B11 + PD7/26	mAb, mouse	Human	IHC	Omnis Dako	*Ready-to-use*
CD3	Dako	GA503	pAb, rabbit	Human	IHC	Omnis Dako	*Ready-to-use*
CD4	Dako	4B12	mAb, mouse	Human	IHC	Omnis Dako	*Ready-to-use*
CD20cy	Dako	L26	mAb, mouse	Human	IHC	Omnis Dako	*Ready-to-use*
PD-1	Cell Marque	NAT105	mAb, mouse	Human	IHC	Ventana (Roche)	1:50
PD-L1	BioLegend	29E.2A3	mAb, mouse	Human	IHC	Manual	1:200
Nitrotyrosine	Abcam	HM.11	mAb, mouse	Human/mouse	IF	Manual	1:25
Myeloperoxidase (MPO)	R&D Systems	AF3174	pAb, rabbit	Human/mouse	IF	Manual	1:25
Nivolumab (anti-PD-1)	Bristol-Myers Squibb	-	humanized mAb	Human/mouse?	IF	Manual	1:200

Immunohistochemistry (IHC), immunofluorescence (IF), monoclonal antibody (mAb), polyclonal antibody (pAb). Markers of NSCLC immunophenotype panel shaded in light gray; other immunohistochemistry markers are shaded in dark gray and immunofluorescence markers are non-shaded

Supplementary Table S2. List of antibodies used for flow cytometry analysis

Protein	Clone	Brand
hCD33	HIM3-4	Becton Dickinson–PharMingen
hCD4	SK3	Becton Dickinson–PharMingen
hCD56	NCAM16,2	Becton Dickinson–PharMingen
hCD19	HIB19	Becton Dickinson–PharMingen
hCD8	SK1	BioLegend
hCD3	UCHT1	Becton Dickinson–Horizon
hCD45	2D1	Becton Dickinson–PharMingen
7-AAD	–	BioLegend
mCD45.1	A20	BioLegend
mLy6G	1A8	BioLegend
mNK1.1	PK136	BioLegend
mCD11B	M1/70	BioLegend
mCD3	145-2C11	BioLegend
mCD45	30-F11	BioLegend

Supplementary Table S3. Antibodies per tube and per tumor homogenate sample used for flow cytometry analysis based on fluorophore labeling.

	FITC	PE	PerCP	PE-Cy7	APC	APC-Cy7	PB	AC
Peripheral blood tube	hCD33	mCD45.1	hCD4	hCD56	hCD19	hCD8	hCD3	hCD45
Tumor tube 1	hCD4	mCD45.1	7-AAD	hCD56	hCD19	hCD8	hCD3	hCD45
Tumor tube 2		mLy6G	7-AAD	mNK1.1	mCD11b	mCD3		mCD45
Isolated neutrophil tube	mCD206	mCD11c	7-AAD	mF4/80	mCD11b	mLy6G	mLy6C	mCD45

Abbreviations: FITC (Fluorescein isothiocyanate); PE (Phycoerythrin); PerCP-CY7 (Peridinin chlorophyll protein); PE-Cy7 (Phycoerythrin cyanin 7); APC (Allophycocyanin); APC-Cy7 (Allophycocyanin-cyanin 7); PB (Pacific blue); AC (AmCyan).

Supplementary Table S4. Antibody conditions for immunofluorescence staining.

	Primary antibody			Secondary antibody		
		Dilution	**Supplier**		**Dilution**	**Supplier**
Myeloperoxidase	anti-MPO	1:25	R&D Systems	anti-goat IgG Alexa 546	1:500	Invitrogen
Nitrotyrosine	anti-Nitrotyr	1:25	Abcam	anti-mouse IgG Alexa 488	1:500	Invitrogen
PD-1	anti-PD-1	1:200	Bristol-Myers Squibb	anti-human IgG Alexa 546	1:500	Invitrogen
Double immunofluorescence:	anti-MPO	1:25	R&D Systems	anti-goat IgG Alexa 546	1:500	Invitrogen
Myeloperoxidase/Nitrotyrosine	anti-Nitrotyr	1:25	Abcam	anti-mouse IgG Alexa 488	1:500	Invitrogen
Double immunofluorescence:	anti-MPO	1:25	R&D Systems	anti-goat IgG Alexa 488	1:500	Invitrogen
Myeloperoxidase/PD-1	anti-PD-1	1:200	Bristol-Myers Squibb	anti-human IgG Alexa 546	1:500	Invitrogen
Double immunofluorescence of isolated neutrophils: PD-1/FcγR	anti-PD-1	1:20	Bristol-Myers Squibb	anti-human IgG–FITC	1:200	A. Menarini Diagnostics
	PD-1–PE	1/500	Abcam			
Control double immunofluorescence of isolated neutrophils: PD-1/FcγR	hIgG4	1:20	Crown Bioscience, Inc.	anti-human IgG–FITC	1:200	A. Menarini Diagnostics
	PD-1–PE	1/500	Abcam			

Supplementary Table S5. Clinical and pathologic characteristic of patients and passagable lung cancer

ID/No.	Gender	Smoking status	Age	Pathology	Localization	Grade / differenciation	Type	Mutation	Tumor-stage	Established Xenograft
PDX1	M	YES	78	SQC	RUL	Moderately	Infiltrating	NO	pT2a N0 L0 V0 R0 (IB)	YES
PDX2	M	YES	66	SQC	RUL	Poorly	Infiltrating / keratinized	NO	pT2a N0 L1 V1 R0 (IB)	YES
PDX3	M	YES	73	SQC	RUL	Poorly	Non-infiltrating	NO	pT2b N0 (IB)	YES
PDX4	M	YES	79	SQC	ML, RLL	Poorly	Infiltrating / basaloid	NO	pT2a N1 L1 V0 R0 (IIA)	YES
PDX5	M	YES	68	SQC	LLL	Moderately	Infiltrating	NO	pT4 N1 M0 (IIIA)	NO
PDX6	M	NO	62	SQC	LUL	Poorly	Infiltrating / basaloid	NO	pT1b N0 L0 V0 R0 (IA)	YES
PDX7	M	YES	71	SQC	RUL	Moderately	Infiltrating / keratinized	NO	pT3 N1 R0 (IIIA)	YES
PDX8	M	YES	74	SQC	RUL	Poorly	Infiltrating / keratinized	NO	pT2b N1 P0 V0 R0 (IIB)	YES
PDX9	M	YES	55	ADC	ML	Poorly	Infiltrating	NO	pT2a N0 P3 V2 R0 (IB)	YES
PDX10	M	YES	64	SQC	LUL	ns	Basaloid	NO	pT1b N0 M0 (IA)	YES
PDX11	F	YES	64	ADC	RUL	ns	Infiltrating	NO	pT2 N0 L1 V1 R0 (IB)	NO
PDX12	F	NO	80	ADC	RLL	ns	Infiltrating	Exon19Del	pT2a N0 M0 (IB)	NO
PDX13	M	YES	65	ADC	RUL	ns	Infiltrating	ALK/EML4	pT2 N2 M0 (IIIA)	NO
PDX14	M	YES	63	SQC	LUL	Poorly	Infiltrating / keratinized	G719X	pT3 N1 L1 V1 R0 (IIIA)	YES
PDX15	M	YES	36	ADC	LUL	ns	Infiltrating	NO	pT2a N0 (IB)	NO
PDX16	F	NO	60	NEC	LLL	Poorly	ns	NO	pT2a N0 L1 V0 R0 (IB)	YES
PDX17	M	NO	74	ADC	RLL	ns	Infiltrating	NO	pT2a N0 M0 L1 (IB)	NO

Abbreviations: M, male; F, female; SQC, squamous carcinoma; ADC, adenocarcinoma; NEC, neuroendocrine carcinoma; RUL, right upper lobe; LUL, left upper lobe; ML, middle lobe; RLL, right lower lobe; LLL, left lower lobe; ns, not specified.